CONF-790348--1

LA-UR-79-876

TITLE: THE (n,p) REACTION AT 60 MeV ON ND-2 TARGETS

AUTHOR(S): N.S.P. King
Los Alamos Scientific Laboratory
Los Alamos, New Mexico 87545

J. L. Ullmann
Crocker Nuclear Laboratory and Dept. of Physics
University of California
Davis, CA

SUBMITTED TO:
To be published in the Proceedings of the Conference on the (p,n) Reaction and the Nucleon-Nucleon Force.

University of California

MASTER

LOS ALAMOS SCIENTIFIC LABORATORY

Post Office Box 1663 Los Alamos, New Mexico 87545

An Affirmative Action/Equal Opportunity Employer

DISTRIBUTION OF THIS DOCUMENT IS UNLIMITED

Form No. 836 R3
St. No. 2629
12/78

UNITED STATES
DEPARTMENT OF ENERGY
CONTRACT W-7405-ENG. 36

EHB

THE (n,p) REACTION AT 60 MeV ON N>Z TARGETS

N.S.P. King
Los Alamos Scientific Laboratory
Los Alamos, New Mexico

J.L. Ullmann
Crocker Nuclear Laboratory and Department of Physics
University of California, Davis California

1. Introduction:

Historically, the work of Obu & Terasawa[1] and Measday [2] provided evidence that the (n,p) reaction showed some selectivity for population of collective states. However, until the recent experiments at UC Davis, no systematic studies with resolution $\leq$ 1 Me V were undertaken. A comparison of the (n,p) reaction on T_o=0 targets with photo nuclear experiments, inelastic electron scattering (particularly, at θ = 180°), radiative pion capture and hadronic probes has revealed considerable sensitivity to known collective ML and El states[3]. These properties of the (n,p) reaction are identical to those of the (p,n) reaction on the same targets since only ΔT=1 is allowed for both. The extension of the (n,p) reaction to $T_o \neq 0$ targets leads to the same isovector (ΔT=1) selection rule. This is not the case for the (p,n) reaction which can populate ΔT=0,±1 states, favoring those with ΔT=1 and ΔT=0. This paper presents results of the (n,p) reaction at 60 MeV on ^{7}Li, ^{9}Be, ^{27}Al, $^{58,60,62,64}Ni$, ^{90}Zr and ^{209}Bi targets.

The emphasis will be on discussing qualitative features of the data through a comparison with existing results from other nuclear probes as well as observed properties of the isovector transitions anticipated from known isospin selection rules.

The usefullness of the (n,p) reaction for studying isovector excitations is readily made apparent by examining the isospin dependence in (p,p'), (n,n'),(p,n'), and (n,p) scattering. The transition matrix for the (n,p) reaction contains an interaction potential of the form $V_{eff} = \sum_{i=1}^{A} V \vec{t}_1 \cdot \vec{t}_i \, (1+\alpha\vec{\sigma}_1 \cdot \vec{\sigma}_i)$ where $\vec{t}_1 \cdot \vec{t}_i$ can be expanded in terms of isospin raising and lowering operators between the incident projectile and a target nucleon. This interaction can lead to both isospin and isospin-spin flip transitions. Additional isospin independent terms also contribute to the (pp') and (nn') transitions. The ratio of isospin dependent to independent interaction strength for potentials commonly utilized in shell model calculations is ~ 1/3 so that isoscaler transitions in (pp') and (nn') reactions dominate by ~ 9:1 therefore, in regions where states of different isospin occur the isovector states may be difficult to observe.

The isospin Clebsch-Gordon coefficients obtained by projecting out the dependence associated with the entrance and exit channels for a $\Delta T=1$ transition leads to σ (n,p)= 2σ(pp' or nn').

A more important geometric isospin effect for large T_o is that due to the splitting of a particular multipolarity transition strength into isospin components for a $T_o > 1/2$ target nucleus. Different allowed transitions are indicated in fig.1 as well as their relative strengths[4]. This shows that only the (n,p) reaction has no reduction in strength of the reduced matrix element to the $T_>=T_o+1$ states. If $M_{T>}=M_T=M_{T<}$ the entire, unsplit strength is available to the (n,p) reaction.

Additional factors involving available configurations for $T_>$ vs $T_<$ transition matrix elements will modify the above ratios since the interactions are in general isospin dependent.

2. Experimental Results

The present data were obtained at the Crocker Nuclear Laboratory unpolarized neutron facility [5]. Time of flight restrictions on the incident neutrons allows (n,p) reaction data to be obtained with bombarding neutron energy resolution of $\leq$ 1 MeV FWHM for energies ~60 MeV. Recoil proton energy resolution is also $\leq$ 1 MeV. All of the targets used in the present work were $\leq$50mg/cm2 in thickness and isotopically pure to greater than 99%.

2.1 $^7Li(n,p)^7He$ and $^9Be(n,p)^9Li$

The isovector M1 selectivity found for low momentum transfer in T_o=0 targets should be modified due to the T_o= 1/2 ground states in ^{7}Li and ^{9}Be. In this case a splitting of the $\Delta T=1$ M1 strength to the g.s. is allowed between $T_>$= 3/2 and $T_<$=1/2 components Theoretical calculations[8] indicate most of the M1 strength should be concentrated in the $T_<$ states for both ^{7}Li and ^{9}Be due to less spatial symmetry in the T= 3/2 vs T= 1/2 wavefunctions. This result is nicely confirmed by 180° (ee') data[6]. More recently, Baer[7] pointed out the weak $\Delta T=1$ M1 strength to the T= 3/2 parent analogs in the $^7Li(\pi^-,\gamma)^7He$ and $^9Be(\pi^-,\gamma)^9Li$ data from SIN[7]. Further confirmation of this effect is shown in Figures 2,3 for the (n,p) reaction on ^{7}Li and ^{9}Be. The ground state of ^{7}He ($J^\pi = \frac{3}{2}^-$, $T=\frac{3}{2}$) is the parent analog to the 11.25 MeV state in ^{7}Li. In ^{9}Li the ($3/2^-$, 3/2) g.s. and the 2.69 MeV (1/2-, 3/2) state form parent analogs to the M1 states at 14.4 and 17.0 MeV in ^{9}Be seen in the inelastic electron scattering. The angular distributions for these three states are consistent with an L=2 transfer based on DWBA calculations utilizing a macroscopic form factor.

Microscopic form factor DWBA calculations including exchange terms will be required before a detailed comparison can be made with measured M1 matrix elements. The strength of the ^{9}Li g.s. transition is however, ~.2mb/sr for σ cm $\lesssim 40°$

which is at least an order of magnitude less than observed cross sections for collective M1 strength in the (n,p) reaction data for parent analog M1 transitions for A=6 and 12. Inelastic electron results also indicate a ratio of roughly 10 to 1 for even A vs odd A $T_>$M1 strengths.

Evidence can be seen in fig. 3 for two peaks above a smooth phase space or pre-equilibrium energy distribution centered at 7.5 and ~18 MeV excitation energy. Similar structure has been found in (π^-,γ) data on 1p shell nuclei and interpreted as configurational splitting of the $T_>$giant dipole resonance (GDR). This effect has been predicted by Dogotar et al[8] as having its origins in the fact that $1\hbar\omega$ transitions have different values for core and valence nucleons. The relevant major oscillator shell 1^- transitions for A=9 involve the $1s_{1/2}\rightarrow 1p_{3/2}$ spacing of ~28 MeV and $1p_{3/2}\rightarrow 1d_{5/2}$ spacing of ~16 MeV. The difference of 12 MeV is consistent with the observed splitting of the $T_>$GDR region in the ^{9}Be (n,p)^{9}Li reaction. The corresponding GDR region in ^{9}Be at 22 and 32 MeV may well be obscured in ^{9}Be(p,p') since both $T_<$ and $T_>$ components are populated. This is also the case for photonuclear reaction data.

2.2 ^{27}Al(n,p)^{27}Mg

The ^{27}Al(n,p) reaction provides an example of isovector transitions from a (1/2-,1/2) g.s. in the s-d shell[3]. The results are well summarized in fig. 4 showing an energy spectrum at σ_L=15.5°. This is compared to an ^{27}Al(pp') spectrum[9] at σ_L=15° as well as ^{27}Al(γ,xn) and ^{27}Al(γ,tot) photonuclear spectra[10]. The angular distribution for the peak at 14.4 MeV is consistent with an L=1 transfer and exhausts about 20% of the energy weighted GDR sum rule. A macroscopic form factor is used in a DWBA calculation in a model proposed by Satchler 11) for a Goldhaber-Teller GDR excitation.
Total exhaustion of the GDR sum rule is related to the calculated cross section by

$$\frac{d\sigma}{d\Omega}\Big)_{np} = 2\,\beta^2_{GT}\,\frac{d\sigma}{d\Omega}\,{}_{DWBA\,(pp')}$$

The unobserved strength is quite likely distributed outside the 14.4 MeV peak region similiar to the photonuclear results. The 14.4 MeV peak in ^{27}Mg is the parent analog for a 21.3 MeV excitation in ^{27}Al which is very close to the observed peak in the photonuclear distribution. It is worth noting that the momentum transfer dependence in a photonuclear reaction is different than for the (n,p) reaction at a fixed angle so thatexact correspondence between the two should not be expected.

Although some evidence for M1 strength (L=0 angular distribution) was found below 8 MeV in ^{27}Mg,its lack of concentration in excitation energy makes it difficult to obtain quantitative information. The prominent peak in the ^{27}Al (pp') data is predominately isoscaler quadrupole strength which obscures the GDR region. This shows the advantage of having a probe selective to only isovector transitions in helping to sort out collective excitations.

2.3 ^{58,60,62,64}Ni(n,p)^{58,60,62,64}Co

This series of targets was selected as a means of systematically investigating the N-Z dependence of both the relative $T_>$ GDR strength as well as the $T_>$ vs $T_<$ energy splitting in the target. Ngo-Trong and Rowe[12] have carried out a RPA calculation giving the dipole strength distribution for both $T_>$ and $T_<$ components.

Comparison of (γ,n) and (γ,p) have been the primary source of information for the GDR distribution. The (γ,p) reaction is presumed to be selective to $T_>$ states due to an isospin selection rule inhibiting neutron decay. However, neutron decay of $T_>$ states to the IAS of the daughter can exceed the proton decay[12]. The(n,p) reaction should in principle be much more selective to $T_>$ components.

An energy spectrum from the ^{62}Ni(n,p)^{62}Co reaction at σ_L= 16° for 59.4 MeV neutrons is shown in figure 5. The continuum background is assumed to arise from a 3-body channel involving the particle from the decay of a ^{62}Co excited state and the usual ejectile proton. The continuum therefore has the indicated threshold. A pre-equilibrium model would tend to reduce the contribution above the background by including available unresolved states in ^{62}Co up to the maximum allowed proton energy. The picture for collective states discussed below will not be altered by this except in the absolute overall strength. The result of removing the background in a consistent manner from all the target data at 16° is shown in figure 6. The energy scale has been adjusted to represent analog excitation in the target nucleus by taking the coulomb energy shift and mass differences into account. The calculated Co-Ni excitation shifts are 8.8 MeV, 11.1 MeV, 13.4 MeV, and 15.1 MeV for A=58,60,62 and 64 respectively. The vertical bars are the results from Ngo-Trong and Rowe for $T_>$ GDR strength [12]. Remarkably good agreement is found between the data and calculations for the dipole strength distributions. Angular distributions for the GDR regions have L=1 shapes as well. The fraction of the GDR energy weighted sum rule exhausted for a JS DWBA form factor [11] is also given in figure 6. The location of the $T_>$ vs $T_<$ E1 strength is predicted to be ΔE= U $(T_o+1)/T_o$ MeV by Goulard and Fallieros [4] where the scale factor is related to the isospin symmetry potential. The equation $\Delta E=76\ (T_0+1)/A$ reproduces the approximate location of the weighted average $T_<$ excitation energy when compared with the $T_<$ GDR location [12].

Another obvious feature of the data is the rapid decrease in strength for the region below the 1^- strength as A increases from 58 to 64. An obvious candidate is M1 strength since the predominant contributions are from $1f_{7/2}\rightarrow f_{5/2}$ and $2p_{3/2}\rightarrow 2p_{1/2}$ transitions which are essentially completely blocked for ^{64}Ni and unblocked in ^{58}Ni for the (n,p) reaction. This is since the $\Delta T=1$ transition removes a proton and fills a neutron orbital. Recent (ee') experiments by Lindgren et al [13] have found $T_>$ M1 strength in ^{58}Ni at ~10.5 MeV which exhausts close to 50% of the M1 closure sum rule for ^{58}Ni. Some M1 strength in ^{60}Ni was also located at ~12.1 MeV. This upward shifting of available $T_>$ M1 strength by a few MeV appears to continue up to ^{64}Ni based on the present data. It should be pointed out that (ee') $T_>$ M1 strength is reduced by the isospin geometric factor so that higher weak components are difficult to observe.

The angular distributions for this "M1" region do peak in cross section for low momentum transfer. However, they do not fall off rapidly enough to be pure M1. Since evidence for, $T_>$ 8^- stretched configuration strengths which will not be blocked, have been found overlapping the M1 region [1], one might expect contributions to back angle cross sections.

2.4 ^{90}Zr(n,p) ^{90}Y

The A=90 system is a good testing ground for studying $T_>$ giant multipoles due to the (p,γ) work of Hasinoff et al. [14] locating $T_>$ E1 strenth at 14.4, 16.3, 19.4 and 21.0 MeV in ^{90}Zr and the inelastic electron scattering experiments of Fukuda and Torizuka [15] providing evidence for isovector E2 strength at 17 and 26 MeV and E3 strength from 20 to 30 MeV. A number of theoretical calculations are also available for $T_>$ E1, E2, and E3 energy distributions [16].

A ^{90}Zr (n,p) ^{90}Y spectrum at 16° is shown in figure 7. The smooth curve is the 3-body phase space assumed for a background. The subtracted data is given in figure 8 with the observed $T_>$ E1 strength from (p,γ) and E2 strength from (ee') shown as solid and dotted lines respectively. The corresponding energies in ^{90}Y were obtained by subtracting 13.3 MeV from the ^{90}Zr energies. The overall E1 energy distribution is not too different from that obtained from the photonuclear data[14], however some contribution from higher multipoles is evident in the angular distribution for the proton energy region above 40 MeV.

This should be expected based on the E2 strength from the (ee') data. In addition, the observed cross section of 6.5 mb/sr at 16° is 54% larger than that required to exhaust the GDR sum rule. The angular distribution for Ep = 40 to 30 MeV (~12 MeV excitation is 90Y) is consistent with an L transfer of greater than one. This region has an analog in ^{90}Zr at 25.3 MeV where Fukuda and Torizuka found considerable isovector E2 strength. The possibility for isovector E3 strength cannot be ruled out based on energy systematics or the angular distributions.

2.5 $^{209}Bi(n,p)^{209}Pb$

Three experiments prompted the investigation of the $^{209}Bi(n,p)$ reaction;1) the indication of $T_>$ E2 strength in ^{209}Bi from the $^{208}Pb(p,\gamma)^{209}Bi$ work of Snover et al.[17]) and 2) the subsequent location of a peak in ^{209}Pb at ~ 7.9 MeV close to the excitation energy of the parent analog to the same resonance via ^{209}Bi (π^-,γ) ^{209}Pb,[18]) and 3) the collective E2 strength found in ^{208}Pb (ee') data between Ex ~ 18 to 27 MeV [19]). The energy spectrum in figure 9 shows a peak at 7.5 MeV which would have an analog at 26.3 MeV.

Since most of the neutron orbitals are full for simple $1\hbar\omega$ transitions in A=209 only very weak parent analogs to the GDR of ^{209}Bi are possible. Few $2\hbar\omega$ M1 transitions are available so that little M1 strength is expected. The excitation energy is consistent with that for parent analogs to collective isovector E2 excitations at 120/A(1/3) = 20 MeV. The angular distribution is given in figure 10 with a DWBA calculation utilizing a JS form factor exhausting 100 % of the isovector E2 sum rule as calculated by Brown and Madsen [20]). The calculated strength is based on the known isoscaler E2 strength from ^{209}Bi (pp') isoscaler E2 measurements [21]) and assumes $|V_1/Vo| \sim 1/2$ for isovector to isoscaler potential strengths.

3.0 Conclusions

The $^7Li(n,p)^7He$ and $^9Be(n,p)^9Li$ reactions both show evidence for population of parent analogs to well known M1 transitions in the target nuclei. Configuration splitting of the GDR for A=9 was also found in agreement with (π^-,γ) data.

For $A \geq 27$, enhancements over a continuum background are consistent with parent analog E1 and E2 states. The results are much less dramatic than for the $T_o=0$ targets and angular distributions are not uniquely fitted by one L transfer. The geometric isospin factors favoring $\Delta T=1$ (n,p) transitions do provide an advantage over inelastic (pp'),(nn'),or (ee') scattering and (p,n) reactions for investigating $T_>$ isovector giant multipole states. The Ni isotope data provides perhaps the best example to be found of $T_>$ GDR population as a function of N-Z with fixed Z for comparison with theory. The additional complexity of possible overlapping isovector multipole states in Zr and Bi make interpretation of the data more difficult.

Since the strength of $T_>$ states is related to isoscaler states via the ratio of the isovector to isoscaler interaction potentials [20] and the location of these states is proportional to the isospin symmetry potential [4] the (n,p) reaction forms a unique tool for investigating isospin dependence in the effective nuclear interaction potential.

The authors would like to acknowledge F.P. Brady, D.H. Fitzgerald, M.W. McNaughton, G. Needham, J.L. Romero, T.S. Subramanian, J. Wang, and C. Zanelli for their many contributions in obtaining the data presented here.

References

1. M. Obu & T. Terasawa Prog. Theor. Phys. 43 (1970) 1231
2. D.F. Measday & J.N. Palmieri Phys. Rev. 161 (1967) 1071
3. UCD Progs. Reports, Brady et al. PRL 36 (1976) 15
4. S. Fallieros & B. Goulard Nuc. Phys.A147 (1971) 593
5. F.P. Brady et al., NBS SP425 (1975) 103 Ed R.A. Schrack and C.D. Bowman
6. L.W. Fagg,Rev. Mod. Phys. 47 (1975) 683
7. H.W. Baer, 7th Int. Cont. on High Energy Physics and Nuc. Structure El. M. Locker, Birkhauser Verlag, Basel (1978)
8. G.B. Dogotar et al.,Nuc. Phys. A282 (1977) 474
9. M.B. Lewis and F.E. Bertrand Nuc. Phys. A196 (1972) 337
10. Atlas of Photoneutron cross sections obtained with Memo energetic Photos B.L. Berman UCRL - 74622
11. G.R. Satchler, Nuc. Phys. A195 (1972) 1
12. C. Ngo-Trong and D.J. Rowe, Phys. Lett. 36B (1971) 553
13. R.A. Lindgren et al., PRC. 14 (1976) 1789
14. M. Hasinoff et al. Nuc. Phys. A216 (1973) 221
15. S. Fukuda and Y. Torizuka, Phys. Lett. 62B (1976) 146
16. J.D. Vergados and T.T.S. Kuo. Nuc. Phys. A168 (1971) 225; T.A. Hughes & S. Fallieros, in Nuc. Isospin, ed. J.D. Anderson, S.P. Bloom J. Cerny, and W.W. True (Acad. Press, N.Y. 1969) p109
17. K. Snover et al.,PPL 32 (1974) 317
18. H. Baer et al.,PRC 10 (1974) 267
19. M. Sasao and Y. Torizuka PRC 15 (1977) 217
20. V. Brown and V. Madsen PRC 17 (1978) 1943
21. F. Bertrand Ann. Rev. Nuc. Sci. 26 (1976) 457

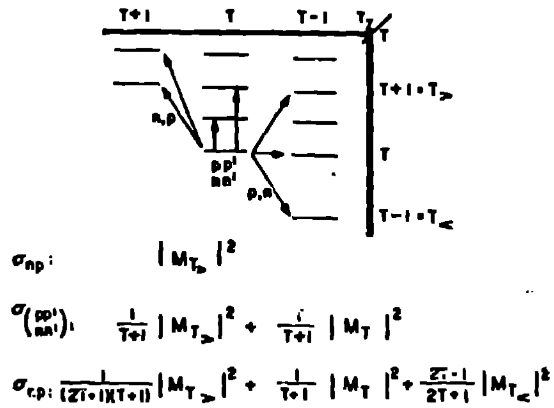

figure 1

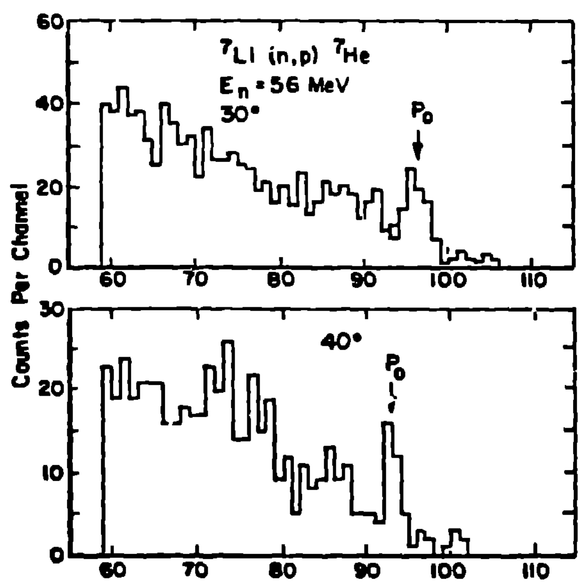

figure 2

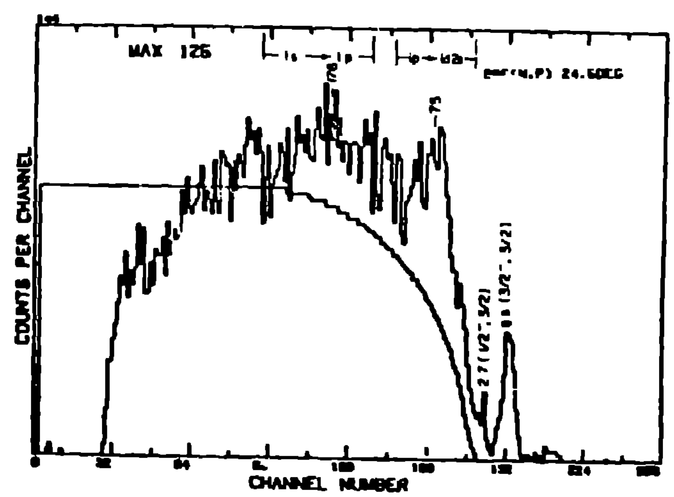

figure 3

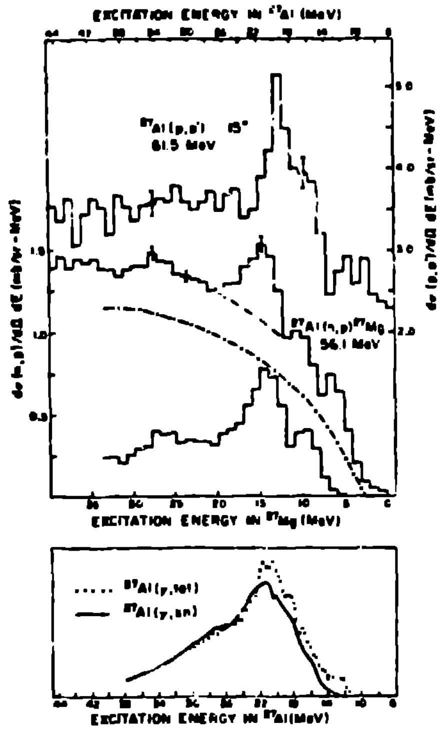

figure 4

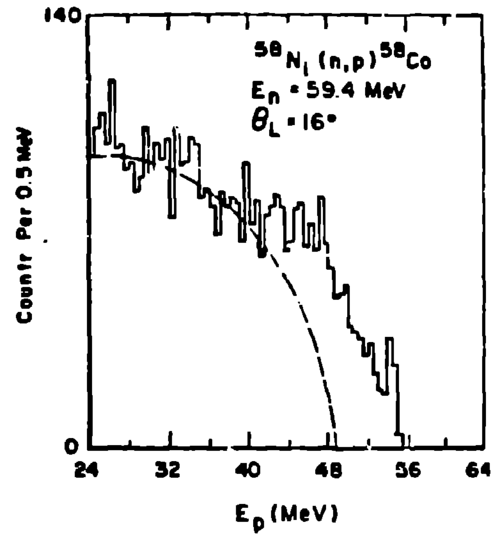

figure 5

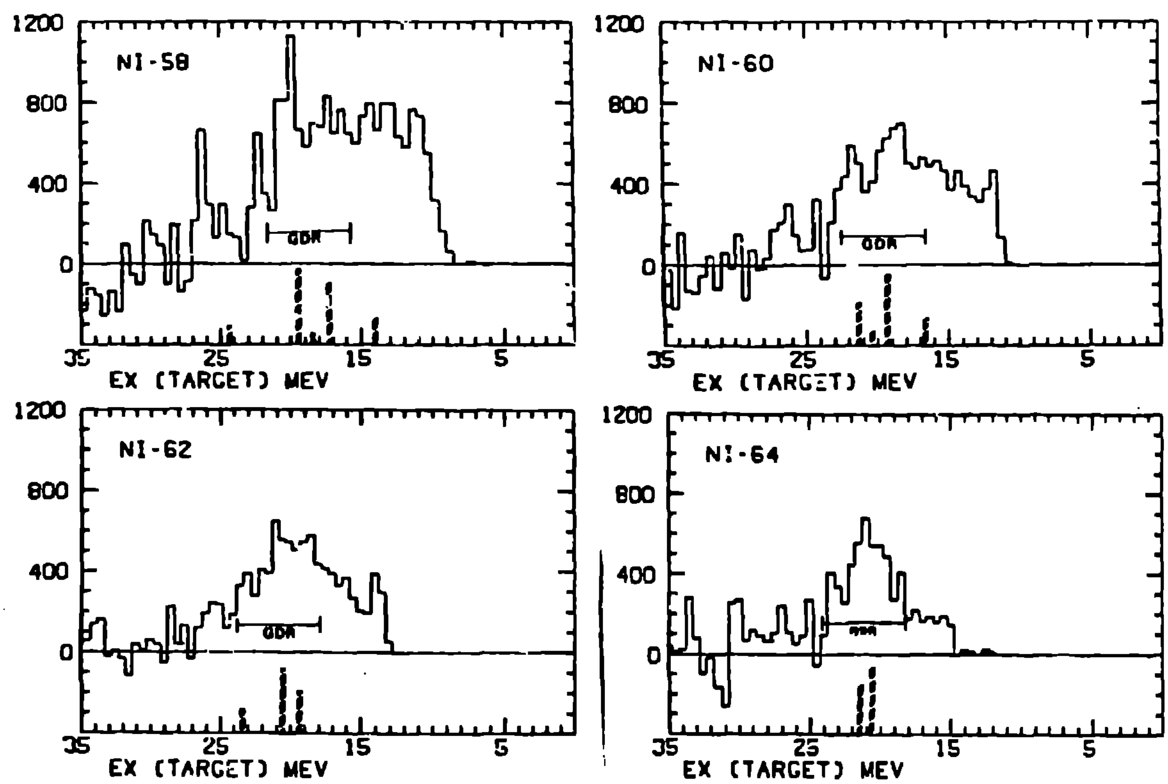

figure 6

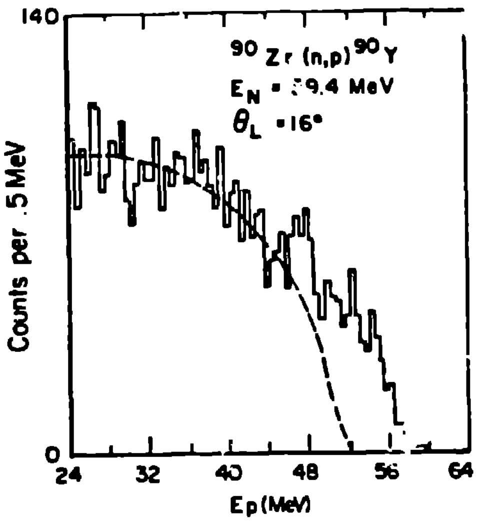

figure 7

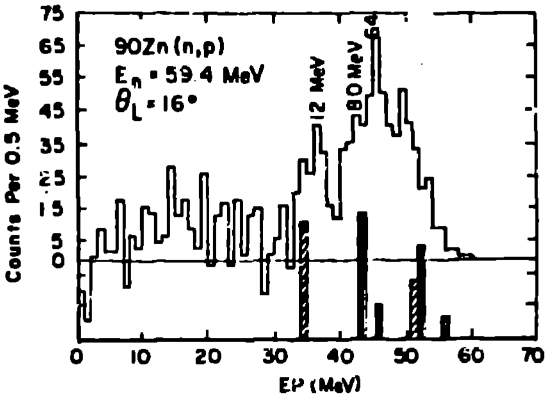

figure 8

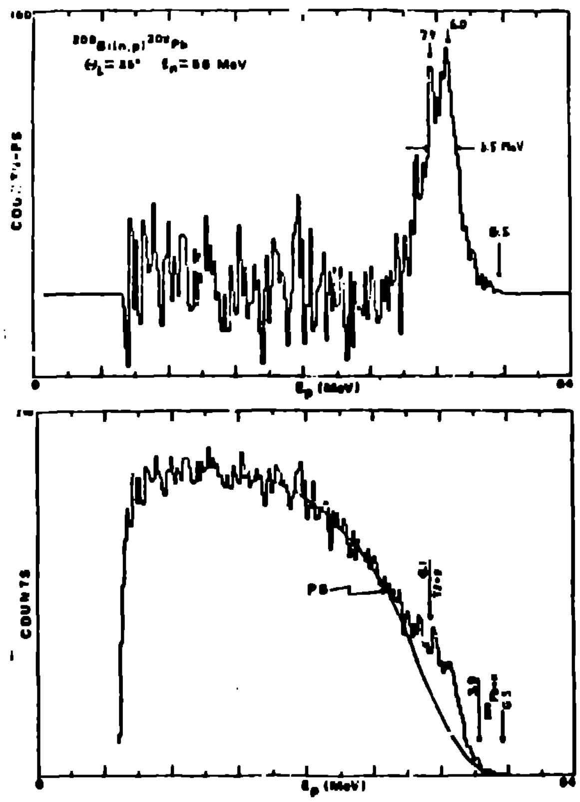

figure 9

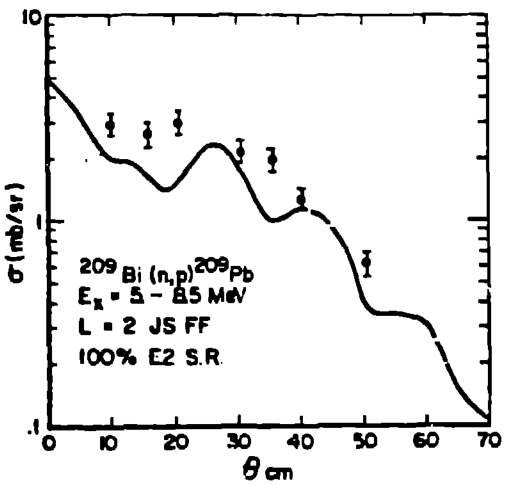

figure 10